

PHASE DIAGRAM FOR THE HEXAGONAL ISING LATTICE

M. Kaburagi,^{a)} T. Tonegawa^{b)} and J. Kanamori^{c)}

a) College of Liberal Arts, Kobe University, Tsurukabuto, Nada, Kobe 657, Japan b) Department of Physics, Faculty of Science, Kobe University, Rokkodai, Kobe 657, Japan c) Department of Physics, Faculty of Science, Osaka University, Toyonaka 560, Japan

A magnetic phase diagram for the simple hexagonal Ising lattice is calculated by use of the cluster variation method. The effect of the interaction between adjacent sites along the hexagonal axis (the intrachain interaction) is investigated. An existence of the antiferromagnetic intrachain interaction changes considerably the characteristics of the phase diagram, whereas that of the ferromagnetic one does not. The temperature dependence of sublattice magnetizations is also calculated.

1. Introduction

The Ising model on a simple hexagonal lattice is of theoretical and experimental interest because it provides a phenomenological model for ordering phenomena in a variety of substances. A typical example is a magnetic ordering in CsCoCl₃ [1] and CsCoBr₃ [2]. Another example is an ordering of interstitial atoms in metals with hexagonal close-packed structure [3]. It is sometimes convenient to regard the lattice as a regular stack of the basal planes of the triangular lattice or as a set of chains along the hexagonal axis which form the triangular lattice. We use the terms "intraplane" and "intrachain" rather than the terms "interchain" and "interplane". This paper deals with the simple hexagonal Ising lattice with the intrachain nearest-neighbor (nn) interaction J₀, the intraplane nn interaction J₁ and the intraplane next-nearest-neighbor (nnn) interaction J₂ in the presence of an external magnetic field H. The Hamiltonian of the present system is given by

$$H = J_1 \left(\alpha_0 \sum_{\lambda i} \sum_{\lambda i} \sigma_{\lambda i} \sigma_{\lambda+1i} + 2 \sum_{\lambda ij} \sum_{\lambda ij} \sigma_{\lambda i} \sigma_{\lambda j} + \alpha \sum_{\lambda ik} \sum_{\lambda ik} \sigma_{\lambda i} \sigma_{\lambda k} - 2h \sum_{\lambda i} \sigma_{\lambda i} \right) \quad (J_1 > 0), \quad (1)$$

where the suffix λ refers to the basal plane; the suffices i, j and k refer to the sites of the triangular lattice in the basal plane; $\sigma_{\lambda i}$ is the Ising spin operator at the site specified by λ and i , taking the value $+1$ or -1 ; α_0 and α are the ratios of $2J_0$ and $2J_2$ to J_1 , respectively; h is the reduced magnetic field defined by $h = \mu H / 2J_1$, μ being the magnetic moment of a single spin; the sum over i and j in the second term and that over i and k in the third term are taken over all intraplane nn and intraplane nnn pairs of sites, respectively. Throughout this paper, we assume that J_1 is positive (antiferromagnetic) and J_2 is negative (ferromagnetic). The sign of J_0 is either positive or negative.

The finite temperature problem for the $J_0=0$ case (the triangular Ising lattice) has been discussed by many authors. Mekata has examined the $J_0=H=0$ case within the molecular field approximation (MFA) and has shown that the paramagnetic (P), partially disordered (PD), three-sublattice ferrimagnetic (3FR) and two-sublattice ferrimagnetic (2FR) phases appear successively with decreasing temperature [4]. However, recent results of the Monte Carlo calculation by Wada et al. [5] and those of the application of the cluster variation method (CVM) [6] by the present authors [7] suggest that the PD and 3FR phases are not thermodynamically stable phases. On the other hand, neutron scattering measurements on CsCoCl₃ and CsCoBr₃ have demonstrated that there exists a temperature region where the PD phase appears [1,2]. Therefore, it is expected that the intrachain

interaction, which is predominant in CsCoCl_3 and CsCoBr_3 , may promote the stability of the PD phase. Shiba has carried out a calculation for the $J_0 > 0$ and $H=0$ case by treating the intrachain interaction exactly and the intraplane (interchain) interactions within the MFA and has shown that Mekata's picture of the successive phase transitions is not changed so much [8].

The purpose of this paper is to calculate a magnetic phase diagram of the system described by the Hamiltonian (1). We also aim at investigating the effect of the intrachain interaction on the phase diagram, focusing our attention on the stability of the PD phase. In §2, the ground state is analysed by use of the method of inequalities [9] to find the type of ordered phases which must be stable at low temperatures. In §3, we calculate the phase diagram with the six-sublattice model shown in Fig. 1 by applying the CVM [6]. Calculations are carried out within the intraplane nn equilateral triangle plus intraplane nnn equilateral triangle plus intrachain nn pair approximation (TTPA). It is shown that the antiferromagnetic intrachain interaction promotes the stability of the PD phase, whereas the ferromagnetic one does not. The temperature dependence of sublattice magnetizations is also calculated. Concluding remarks are given in §4.

2. Ground State

The ground state of the present system can be determined rigorously by the method of inequalities [9]. In what follows, we assume $h \geq 0$. It is shown that four phases can appear in the ground state. The spin structures of these phases are expressed in the following way. We first decompose the triangular lattice in the basal planes into three sublattices, called the A, B and C sublattices, as shown in Fig. 1. Then, we have eight types of the basal planes with spin configurations specified by $(\sigma_A, \sigma_B, \sigma_C)$ as a: $(-1, +1, +1)$; b: $(+1, -1, +1)$; c: $(+1, +1, -1)$; f: $(+1, +1, +1)$; \bar{a} : $(+1, -1, -1)$; \bar{b} : $(-1, +1, -1)$; \bar{c} : $(-1, -1, +1)$; \bar{f} : $(-1, -1, -1)$. The spin structures of the above four phases are eventually represented by stacking sequence of the planes as (i) -f-, (ii) -a-b-, -a-b-c-, etc., (iii) -a- \bar{a} - and (iv) -a-, where we list repeating units and non-equivalent structures only. It should be noted that there are infinite numbers of degenerate spin structures in phase (ii) because the structures in which each plane is of a, b or c type and adjacent planes are of different types have the same energy. When $J_0 > 0$ ($\alpha_0 > 0$), phases (iii), (ii) and (i) appear for $0 \leq h < h_{C1} = \alpha_0$, $h_{C1} < h < h_{C2} = \alpha_0 + 6$ and $h_{C2} < h$, respectively. When $J_0 < 0$ ($\alpha_0 < 0$), phases (iv) and (i) appear for $0 < h < h_{C3} = 6$ and $h_{C3} < h$, respectively. In the latter case, $h=0$ is a phase boundary at which the -a- to - \bar{a} - first-order phase transition occurs.

We consider here a decomposition of the lattice into sublattices. Because of the degeneracy of phase (ii), we have no sublattice model which can reproduce all of the spin structures appearing in the ground state. The simplest model which can reproduce the spin structures of phases (i), (iii) and (iv) and some of those of phase (ii) is the six-sublattice model shown in Fig. 1. In the model, the basal planes are classified into two subplanes, namely, the X and Y subplanes, where we refer to a set of every second plane as X and another set of the remaining planes as Y. The above spin structures can be written as (i) X=Y=f, (ii) X=a, Y=b, (iii) X=a, Y= \bar{a} and (iv) X=Y=a. With this classification, the hexagonal lattice is decomposed into six sublattices, called the XA, XB, XC, YA, YB and YC sublattices. This six-sublattice model, though it is inadequate to deal with the degeneracy of phase (ii), will be used in the calculation of the phase diagram in the next section.

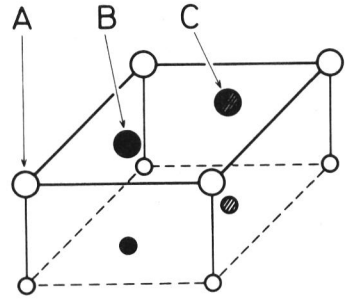


Fig. 1. Classification of the basal planes and decomposition of the triangular lattice in the basal planes. Large and small circles are lattice sites on the X and Y subplanes, respectively. Open, full and shaded circles correspond, respectively, to the A, B and C sublattices in each subplane.

3. Phase Diagram

We now turn to the calculation of the phase diagram by use of the CVM [6]. In the calculation, we employ the TTPA mentioned in the Introduction. It is noted that the TTPA gives the exact results for the $J_1=J_2=0$ case (the linear chain) and the TTA results obtained in ref. 7 for the $J_0=0$ case (the triangular lattice). Adopting the six-sublattice model discussed in the previous section, we have twenty-nine variational parameters. These are six sublattice magnetizations, denoted as x_{XA} , x_{XB} , x_{XC} , x_{YA} , x_{YB} and x_{YC} , and correlation functions associated with six intraplane nn pairs,

six intraplane nnn pairs, three intrachain nn pairs, two intraplane nn triangles and six intraplane nnn triangles. Minimization of the free energy with respect to the above variational parameters leads to a set of twenty-nine simultaneous non-linear equations which determine these parameters. Using the method discussed in ref. 7, we have solved the equations with $\alpha(=2J_2/J_1)$ fixed at -0.2 and with $\alpha_0(=2J_0/J_1)$ at -6.0 or $+6.0$. In the following discussions, we use the reduced temperature t defined as $t=k_B T/2J_1$, k_B being the Boltzmann constant.

When $h=0$, we can derive four non-equivalent solutions for both the $\alpha_0=-6.0$ case and the $\alpha_0=+6.0$ case. The sublattice magnetizations in these four solutions are represented by using three order parameters, x_1 , x_2 and x_3 , as $(x_{XA}, x_{XB}, x_{XC})=\pm(x_{YA}, x_{YB}, x_{YC})=(x_1, x_2, x_3)$, where the upper and lower signs correspond to the $\alpha_0=-6.0$ and $\alpha_0=+6.0$ cases, respectively; the four solutions are characterized as (I) $x_1=x_2=x_3=0$, (II) $x_1=-x_3>0$, $x_2=0$, (III) $x_1>x_2>0$, $x_3<0$ and (IV) $x_1=x_2>0$, $x_3<0$, which correspond, respectively, to the P, PD, 3FR and 2FR phases mentioned in the Introduction. Therefore, we refer to solutions (I), (II), (III) and (IV) as the P, PDI (PDII), 3FRI (3FRII) and 2FRI (2FRII) phases, respectively, for the $\alpha_0=-6.0$ ($\alpha_0=+6.0$) case. In the $\alpha_0=-6.0$ ($\alpha_0=+6.0$) case, the P to PDI (PDII), PDI (PDII) to 3FRI (3FRII) and 3FRI (3FRII) to 2FRI (2FRII) second-order phase transitions have been found to occur, respectively, at $t=t_{N1}=6.959$, $t=t_{N2}=4.549$ and $t=t_{N3}=4.534$. The temperature dependence of the order parameters x_1 , x_2 and x_3 for the $|\alpha_0|=6.0$ cases is shown in Fig. 2.

In Fig. 3(a), we show the resulting phase diagram for $\alpha=-0.2$ and $\alpha_0=-6.0$ in the (h,t) plane, representing the regions where each of four phases is stable. The regions are called by the names of the stable phases. The 3FRI region, which is the segment from $t=t_{N2}$ to $t=t_{N3}$ on the t axis surrounded by the PDI region, is not shown in the figure, since the difference between t_{N2} and t_{N3} is so small that it cannot be drawn. Comparing this phase diagram with the one for $\alpha=-0.2$ and $\alpha_0=0$, which is shown in Fig. 7 of ref. 7, we may say that the characteristics of the phase diagram is not changed by the existence of the ferromagnetic intrachain interaction.

Figure 3(b) shows the calculated phase diagram for $\alpha=-0.2$ and $\alpha_0=+6.0$. Although there exists a narrow 3FRII region between the 2FRII and PDII regions, we omit it in the figure, since it is too narrow to be drawn. It is noted that all calculated phase boundary lines, except the low temperature part ($t<2.6$) of the phase boundary line between the 2FRII and 3FRII phases, are second-order phase boundary lines within the numerical accuracy. It is interesting to note that the PDII phase in which the sublattice magnetizations are given as $x_{XA}=x_{YC}$, $x_{XB}=x_{YB}$ and $x_{XC}=x_{YA}$ can be turned continuously into the $-c-a-$ structure of phase (ii) at $t=0$ without undergoing a phase transition. Since the region where the phase corresponding to the PD phase is stable becomes larger, we may say that

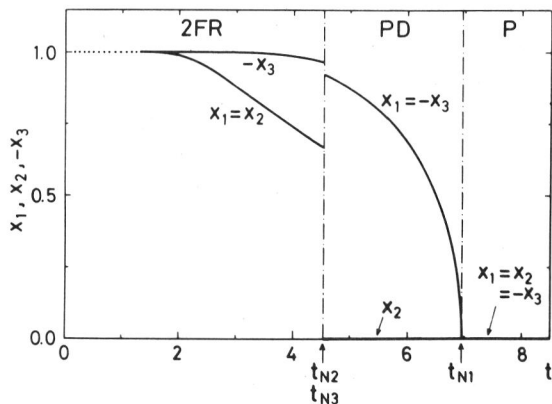


Fig. 2. Dependence on the reduced temperature t of the order parameters x_1 , x_2 and x_3 calculated for $h=0$, $\alpha=-0.2$ and $|\alpha_0|=6.0$.

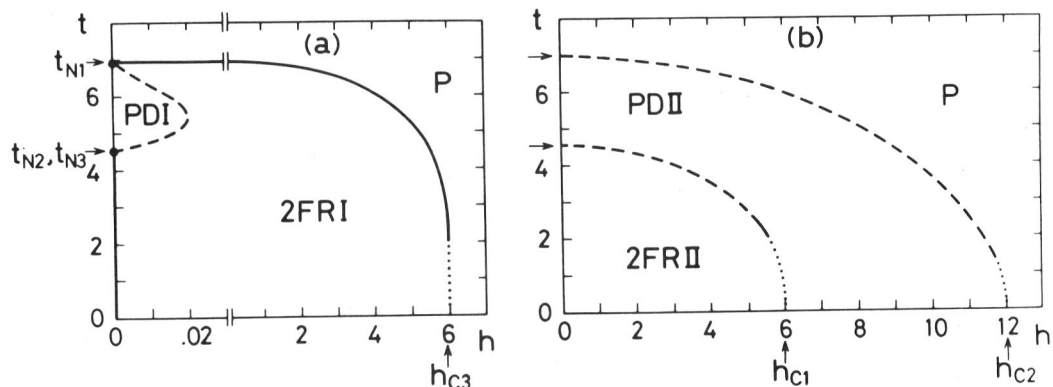


Fig. 3. Temperature versus magnetic field phase diagram obtained for (a) $\alpha = -0.2$, $\alpha_0 = -6.0$ and (b) $\alpha = -0.2$, $\alpha_0 = +6.0$ within the TTPA. The solid and dashed lines represent the calculated phase boundary lines of first-order and second-order transitions, respectively, and the dotted lines show extrapolations to $t=0$. In (a), the 3FRI region, which is a segment from $t=t_{N2}$ to $t=t_{N3}$ on the t axis is omitted. In (b), the narrow 3FRII region between the 2FRII and PDII regions is omitted and the boundary line between the 2FRII and 3FRII phases is shown.

the existence of the antiferromagnetic intrachain interaction promotes the stability of the PD phase.

Although the numerical calculation cannot be performed at very low temperatures, the calculated phase boundary lines shown in Fig. 3 can be extrapolated naturally to $t=0$ in such a way that the results of the ground state analysis in the previous section are reproduced.

4. Concluding Remarks

The phase diagram for the simple hexagonal Ising lattice is calculated by applying the CVM. Calculations are performed within the TTPA. We show that the antiferromagnetic intrachain interaction promotes the stability of the PD phase, whereas the ferromagnetic one does not change the characteristics of the phase diagram. As mentioned before, however, the present six-sublattice model is inadequate to deal with the degeneracy of phase (ii) of the ground state. It is possible that ordered phases with long period modulation appear at low temperatures in the PDII region. Details of this work will be published elsewhere.

References

- [1] M. Mekata and K. Adachi: *J. Phys. Soc. Jpn.* **44** (1978) 806; H. Yoshizawa and K. Hirakawa: *J. Phys. Soc. Jpn.* **46** (1979) 448.
- [2] W. B. Yelon, D. E. Cox and M. Eibschütz: *Phys. Rev. B* **12** (1975) 5007.
- [3] M. Koiwa and M. Hirabayashi: *J. Phys. Soc. Jpn.* **27** (1969) 807.
- [4] M. Mekata: *J. Phys. Soc. Jpn.* **42** (1977) 76.
- [5] K. Wada, T. Tsukada and T. Ishikawa: *J. Phys. Soc. Jpn.* **51** (1982) 1331.
- [6] For a review of the CVM, see for example D. M. Burley: *Phase Transitions and Critical Phenomena*, ed. C. Domb and M. S. Green (Academic, London and New York, 1972) Vol. 2, p. 329.
- [7] M. Kaburagi, T. Tonegawa and J. Kanamori: to be published in *J. Phys. Soc. Jpn.* **51** (1982) No. 12.
- [8] H. Shiba: *Prog. Theor. Phys.* **64** (1980) 466.
- [9] M. Kaburagi and J. Kanamori: *Jpn. J. Appl. Phys. Suppl.* **2**, pt. 2 (1974) 145; *Prog. Theor. Phys.* **54** (1975) 30; *J. Phys. Soc. Jpn.* **40** (1976) 291.